

Thyristor Controlled Based Reactive Power Control for a Grid Voltage Oriented Vector Doubly Fed Induction Machine

Hari Krishnan I

M. Tech (Power Electronics), EEE Dept.
 REVA Institute of Technology and Management
 Bangalore, India
 krishnan.hari380@gmail.com

Ashwini Kumari P

Asst. Prof. EEE Dept.
 REVA Institute of Technology and Management
 Bangalore, India
 kanchanapu@gmail.com

Abstract—Electric power generation through wind turbine is growing rapidly every year and India plays a major role in generating electric power through wind turbine. In India almost 25GW of electric power is being generated every year through wind turbine. Also, wind energy is very clean, reliable and is available by a very vast amount. In this paper, mathematical model of DFIM, back to back converters along with DC link capacitor and a thyristor controlled reactor to adjust the reactive power control of wind turbine has been presented. The wind turbine speed is controlled by controlling the pitch angle control. Grid voltage oriented vector control is used to control the DC link voltage and control the flow of active power to the grid. PWM with third harmonic injection is used to generate switching pulses for the converters. Analysis of DFIM is done in both open and closed loop configurations of converters, at different wind speeds. All the simulation is carried out in Matlab/Simulink.

Keywords- Doubly Fed Induction Machine, Voltage source converter, Pulse width modulation, Thyristor Controlled Reactor.

I. INTRODUCTION

Renewable energy including solar, wind and tidal energies is sustainable, reusable and environmentally friendly and clean. With the increasing shortage in fossil fuels, and pollution problems renewable energy has become an important energy source. Among the other renewable energy sources wind energy has proven to be one of the most economical one. Earlier Constant speed WECS were proposed to generate constant frequency voltages from the variable wind. However, Variable speed WECS operations can be considered advantageous over other renewable energy sources and especially because of additional energy can be collected as the wind speed increases.

Three types of machines are used as generators in WECS namely Cage induction motors, doubly fed induction generators and permanent magnet synchronous generators. Out of these three generators DFIG's are the most frequently used generators. This is because of the fact that DFIG's are efficient, robust and flexible for wind energy applications. A doubly fed induction machine is basically a standard, wound rotor induction machine with its stator windings directly connected to the grid and its rotor windings connected to the grid through converters.

In this paper, first, the classic and commonly used two-level voltage source converters (VSC) is described, its mathematical model is developed and is examined. Pulse width modulation with third harmonic injection (PWM THI) is adopted to provide switching functions for the converter's switches. The converter developed can be used for both rotor and grid side converter

II. DFIM BASED WIND TURBINE

Fig. 1 shows the system configuration of DFIM based wind turbine. It consists of a wind turbine connected to the DFIM through a gearbox and a shaft. The speed of the wind turbine can be controlled by changing the pitch angle of the blades; this is called Pitch angle control. This control can only be done up to some extent. If in case there is a wind gust, in order to protect the whole system and to avoid the transfer of vibration

from mechanical to electrical system the wind turbine is detached from the DFIM.

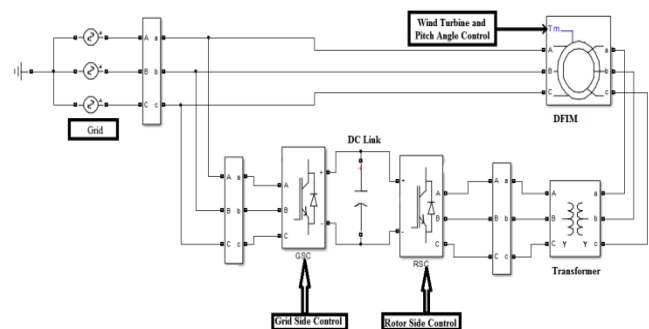


Figure 1. DFIM based WT

DFIM works as a motor in sub synchronous speeds and as generator in super synchronous speeds.

As it can be seen there are two controllers, rotor side controller (RSC) and grid side controller (GSC). RSC is connected to rotor of DFIM and GSC is connected directly to the grid. These two controllers are connected by a DC link. DC link (capacitor or any energy storing unit used in power system) is used to maintain constant voltage in its terminals.

The switching signals given to switches of these controllers are by sinusoidal PWM technique. In this technique a reference sinusoidal signal is compared with a triangular signal and pulses are generated when the amplitude of sine wave goes higher than that of triangular wave. In order to increase the efficiency of the converters, third harmonic is injected into the sine wave used PWM control.

Applying KVL to the fig. 2 the stator and rotor voltages are

$$V_s(t) = R_s I_s(t) + \frac{d\Psi_s(t)}{dt} \quad (1)$$

$$V_r(t) = R_r I_r(t) + \frac{d\Psi_r(t)}{dt} \quad (2)$$

$$\Psi_s(t) = L_s I_s(t) + L_m I_r(t) \quad (3)$$

$$\Psi_r(t) = L_r I_r(t) + L_m I_s(t) \quad (4)$$

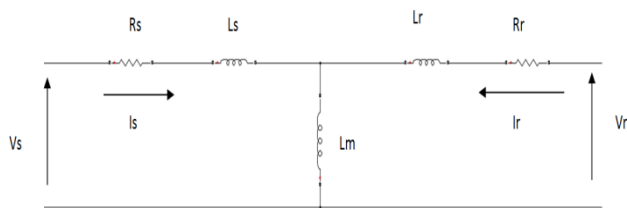


Figure 2. Equivalent circuit for the DFIM

Representing the currents in α - β coordinates

$$\frac{d}{dt} \begin{bmatrix} I_{\alpha s} \\ I_{\beta s} \\ I_{\alpha r} \\ I_{\beta r} \end{bmatrix} = \left(\frac{1}{\sigma L_s L_r} \right) \begin{bmatrix} -R_s L_r & \omega_m L_m^2 & R_r L_m & \omega_m L_m L_l \\ -\omega_m L_m^2 & -R_s L_r & -\omega_m L_m L_r & R_r L_m \\ R_s L_m & -\omega_m L_s L_m & -R_r L_s & -\omega_m L_r L \\ \omega_m L_s L_m & R_s L_m & \omega_m L_r L_s & -R_r L_s \end{bmatrix} \begin{bmatrix} V_{\alpha s} \\ V_{\beta s} \\ V_{\alpha r} \\ V_{\beta r} \end{bmatrix} + \left(\frac{1}{\sigma L_s L_r} \right) \begin{bmatrix} L_r & 0 & -L_m & 0 \\ 0 & L_r & 0 & -L_m \\ -L_m & 0 & L_s & 0 \\ 0 & -L_m & 0 & L_s \end{bmatrix} \begin{bmatrix} V_{\alpha s} \\ V_{\beta s} \\ V_{\alpha r} \\ V_{\beta r} \end{bmatrix} \quad (5)$$

Where, $\sigma = 1 - \frac{L_m^2}{L_s L_r}$ (6)

Where, V and I are voltage and current; Ψ is the flux; L inductor of the windings; R resistance of the windings. Subscript s and r represents stator and rotor components. L_m is the mutual inductance.

III. BACK TO BACK TWO LEVEL VOLTAGE SOURCE CONVERTER

DFIM will operate in both motor and generating mode. In, either modes rotor delivers or receives power. Hence, Back to back converter is required for the control of DFIM based WT. Back to back converter is composed of two bidirectional voltage source converter connected to each other by a DC link capacitor. The converters used can be operated as both rectifier and as an inverter. One converter is connected to stator terminals of DFIM and another one is connected to rotor terminals of DFIM.

A. Two Level Voltage Source Converter

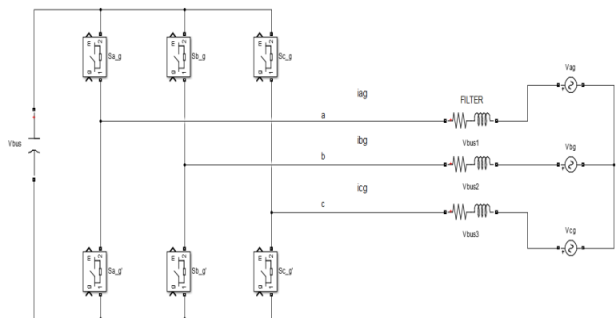


Figure 3. Two levels VSC connected to a grid along with filters

The main condition that must be satisfied is that, no two switches in a leg must conduct.

$$S_j \in \{0, 1\} \text{ And } j = a, b, c \quad (7)$$

From fig. 4. We can write

$$V_{jn} = V_{jo} - V_{no} \quad (8)$$

Assuming the grid voltages to be balanced, we can write

$$V_{an} + V_{bn} + V_{cn} = 0 \quad (9)$$

Substituting eq. 8 in eq. 9 we get

$$V_{no} = \frac{1}{3}(V_{a0} + V_{b0} + V_{c0}) \quad (10)$$

Substituting eq. 10 again in eq. 8 we get the following set of equations.

$$V_{an} = \frac{2}{3}V_{a0} - \frac{1}{3}(V_{b0} + V_{c0}) \quad (11)$$

$$V_{bn} = \frac{2}{3}V_{b0} - \frac{1}{3}(V_{a0} + V_{c0}) \quad (12)$$

$$V_{cn} = \frac{2}{3}V_{c0} - \frac{1}{3}(V_{b0} + V_{a0}) \quad (13)$$

Expressing eq. 11, 12, 13 in terms of switching functions we get

$$V_{an} = \frac{V_{bus}}{3}(2S_{ag} - S_{bg} - S_{cg}) \quad (14)$$

$$V_{bn} = \frac{V_{bus}}{3}(2S_{bg} - S_{ag} - S_{cg}) \quad (15)$$

$$V_{cn} = \frac{V_{bus}}{3}(2S_{cg} - S_{ag} - S_{bg}) \quad (16)$$

Considering the filter, the voltage equations obtained are

$$V_{af} = R_f I_{ag} + L_f \frac{dI_{ag}}{dt} + V_{ag} \quad (17)$$

$$V_{bf} = R_f I_{bg} + L_f \frac{dI_{bg}}{dt} + V_{bg} \quad (18)$$

$$V_{cf} = R_f I_{cg} + L_f \frac{dI_{cg}}{dt} + V_{cg} \quad (19)$$

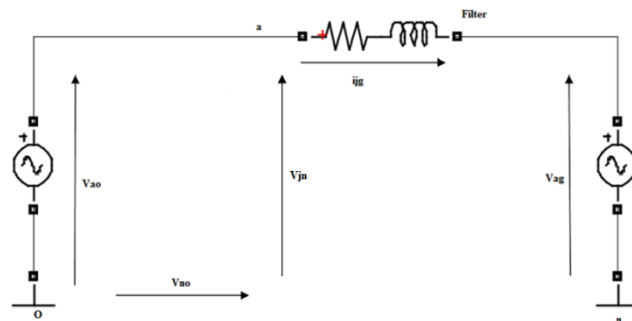


Figure 4. Simplified equivalent single phase circuit

B. DC Link Capacitor

DC link Capacitor connects both the converters, RSC and GSC to form a back to back converter. This capacitor can be a single capacitor or bank of capacitors. The energy stored in this DC link capacitor and this energy is used to supply constant voltage to both the converters throughout the operation of wind turbine. Due to this the efficiency of the converters is also increased.

The DC link voltage is given by eq. 20

$$V_{bus} = \frac{1}{C_{bus}} \int I_c dt \quad (20)$$

Let us assume that the DFIM is working in motoring mode. The power is drawn through rotor terminals. And thus we can consider DC link system as shown in fig. 5. In derivation I_r is taken negative because, while modeling it is considered that

the DC link capacitor is charged to its maximum capacity and is providing constant voltage to Rotor terminals through RSC.

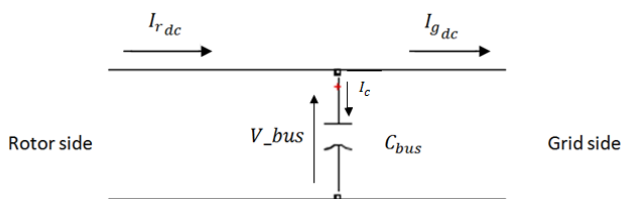


Figure 5. DC Link Capacitor

From the fig. 5

$$I_c = I_{r_{dc}} - I_{g_{dc}} \quad (21)$$

Expressing DC currents in terms of switching functions of RSC and GSC,

$$I_{g_{dc}} = S_{a_g} I_{a_g} + S_{b_g} I_{b_g} + S_{c_g} I_{c_g} \quad (22)$$

$$I_{r_{dc}} = -S_{a_r} I_{a_r} - S_{b_r} I_{b_r} - S_{c_r} I_{c_r} \quad (23)$$

C. Sinusoidal PWM with Third Harmonic Injection

Pulse Width Modulation (PWM) as the name suggests that the width of the pulse is modulated. PWM is the method used to generate switching functions, to make on and off the switches in VSC. The control method adopted to achieve PWM operation is Sinusoidal PWM. In Sinusoidal PWM, the amplitude a reference sine wave is compared to the amplitude of triangular wave. And when the amplitude of sine wave is greater than triangular wave, a pulse is generated. This condition can be expressed as switching function in eq. 24

$$S_j = 1 \text{ if } V_j^* > V_{tri} \quad (24)$$

To choose the amplitude and frequency of the triangular wave, two factors must be taken into consideration. Those are frequency modulation index and amplitude modulation index.

Frequency modulations index the ratio of frequency of triangular wave to reference sinusoidal wave.

$$m_f = \frac{f_{tri}}{f_{ref}} \quad (25)$$

Amplitude modulation index is the ratio of amplitude of reference sine wave to triangular wave. The range of m_a varies from 0 to 1.15.

$$m_a = \frac{|V^*|}{|V_{tri}|} \quad (26)$$

Sinusoidal PWM technique is very simple. But, DC bus supply voltage is not utilized fully. Hence, third harmonic signal is injected to each of the reference sinusoidal signal. Due to this, the resultant signal obtained will have more width and the gate pulses generated will be longer time increasing the amplitude of the output voltage improving the overall efficiency of the converters. Third harmonic can be injected directly by comparing the amplitude of the reference signals and by using the eq. 27

$$V_3 = -\frac{\max\{V_a^*, V_b^*, V_c^*\} + \min\{V_a^*, V_b^*, V_c^*\}}{2} \quad (27)$$

Where S is switching signals; V_g is grid voltage; I_g grid currents; V_f converter output voltage; R_f converter filter resistance; L_f converter filter inductance; V_{bus} DC link voltage; C_{bus} DC link capacitance; m_f frequency modulation index; f_{tri} frequency of carrier signal; f_{ref} frequency of reference signal; m_a amplitude modulation index; V_{ref} amplitude of reference signal; V_{tri} amplitude of carrier signal.

IV. CONTROL OF VOLTAGE SOURCE CONVERTER

A. Grid Voltage Oriented Vector for GSC

Any three phase quantities can be transformed into any of the three space vector, such as stationery reference frame (α - β), rotating reference frame (D-Q) and synchronous reference frame (d-q). The angular speed with which the complex form of grid voltage rotates is ω_s at 50Hz.

The principle of Grid Voltage Oriented Vector Control (GVOVC) for GSC is that making $\omega_a = \omega_s$ and aligning the reference signal with grid voltage.

The parameters that are being controlled in GVOVC are DC Link Voltage: DC link Voltage is controlled to make sure that V_{dc} is always available for the converters to perform well and to control the active power flow through the converters to the grid and Reactive power exchange with the grid.

The controller measures all the grid voltages and currents, DC link capacitor voltages. DC link Capacitor voltage measured with the reference value and the error measured is controlled by PI controller. The active power exchange of the converter with the grid is directly proportional to this DC link capacitor voltage. The frequency and phase of the grid voltage is measured by the Phase Locked Loop (PLL) control. Finally on conversion of reference signals from $\alpha - \beta$ coordinates to ABC coordinates it is oriented with the grid voltage.

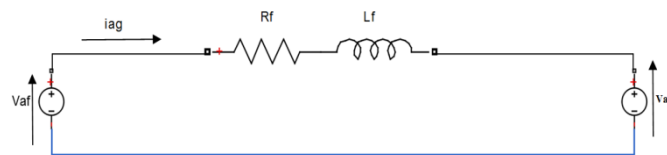


Figure 6. Simplified model of single phase grid system

Applying KVL to fig. 6. We get

$$V_{j_g} = R_f I_{j_g} + L_f \frac{dI_{j_g}}{dt} + V_{j_g} \quad (28)$$

ABC quantities can be converted into $\alpha - \beta$ quantities using Clark direct transformation as shown in eq. 29

$$\begin{bmatrix} V_{\alpha_f} \\ V_{\beta_f} \end{bmatrix} = \frac{2}{3} \begin{bmatrix} 1 & -\frac{1}{2} & \frac{1}{2} \\ 0 & \frac{\sqrt{3}}{2} & -\frac{\sqrt{3}}{2} \end{bmatrix} \begin{bmatrix} V_{a_f} \\ V_{b_f} \\ V_{c_f} \end{bmatrix} \quad (29)$$

Expanding eq. 28 to ABC quantities and using eq. 29 we get

$$V_{\alpha_f} = R_f I_{\alpha_f} + L_f \frac{dI_{\alpha_f}}{dt} + V_{\alpha_g} \quad (30)$$

$$V_{\beta_f} = R_f I_{\beta_f} + L_f \frac{dI_{\beta_f}}{dt} + V_{\beta_g} \quad (31)$$

In general, both eq. 30, 31 can be represented in vector form

$$\vec{V}_f^s = R_f \vec{I}_g + L_f \frac{d\vec{I}_g}{dt} + \vec{V}_g \quad (32)$$

To orient eq. 32 to d-q reference frame multiply all the vectors with $e^{-j\theta}$. We get,

$$\vec{V}_f^s e^{-j\theta} = R_f \vec{I}_g e^{-j\theta} + L_f \frac{d\vec{I}_g e^{-j\theta}}{dt} + \vec{V}_g e^{-j\theta} \quad (33)$$

Consider,

$$\frac{d\vec{I}_g}{dt} e^{-j\theta} = \frac{d\vec{I}_g e^{-j\theta}}{dt} + j\omega_a \vec{I}_g e^{-j\theta} \quad (34)$$

Whereas,

$$\vec{V}_f = V_{d_f} + jV_{q_f} \quad (35)$$

$$\vec{V}_g = V_{d_g} + jV_{q_g} \quad (36)$$

$$\vec{I}_g = I_{d_g} + jI_{q_g} \quad (37)$$

Substituting eq. 34 to 37 in eq. 6.6 we get,

$$V_{d_f} = R_f I_{d_g} + L_f \frac{dI_{d_g}}{dt} + V_{d_g} - \omega_a L_f I_{q_g} \quad (38)$$

$$V_{q_f} = R_f I_{q_g} + L_f \frac{dI_{q_g}}{dt} + V_{q_g} + \omega_a L_f I_{d_g} \quad (39)$$

These voltage signals in d – q coordinates is transformed into ABC coordinates using both Parks and inverse Clark transformation as shown in eq. 40, 41

$$\begin{bmatrix} V_\alpha \\ V_\beta \end{bmatrix} = \begin{bmatrix} \cos\theta & \sin\theta \\ -\sin\theta & \cos\theta \end{bmatrix} \begin{bmatrix} V_d \\ V_q \end{bmatrix} \quad (40)$$

$$\begin{bmatrix} V_a \\ V_b \\ V_c \end{bmatrix} = \begin{bmatrix} 1 & 0 \\ -\frac{1}{2} & \frac{\sqrt{3}}{2} \\ -\frac{1}{2} & -\frac{\sqrt{3}}{2} \end{bmatrix} \begin{bmatrix} V_\alpha \\ V_\beta \end{bmatrix} \quad (41)$$

By putting, $\theta = \theta_s$ in eq. 40 we can orient reference signal with the grid voltage.

B. Rotor Current Reference Vector Control

By rotor current reference vector control, active and reactive power of the stator can be controlled independently. From the error signal measured, the reference signal generated is rotor currents and these currents are compared with the measured rotor currents. The reference signals thus obtained is used to generate the required switching pulses for rotor side converter.

First the relationship between stator powers and rotor currents has to be obtained and for this we can use reference frame aligned with the stator flux. The stator flux vector in eq. 3 can be split into d – q coordinates. Since the reference frame is aligned with the stator flux, the q component can be considered zero. Thus the equation obtained from eq. 3 is as shown in eq. 42, 43.

$$I_{d_s} L_s + I_{d_r} L_m = \Psi_s \quad (42)$$

$$I_{q_s} L_s + I_{q_r} L_m = 0 \quad (43)$$

The active and reactive power of the stator is

$$P_s = \frac{3}{2} V_{q_s} I_{q_s} \quad (44)$$

$$Q_s = \frac{3}{2} V_{q_s} I_{d_s} \quad (45)$$

$$P_s = -\frac{3}{2} V_{q_s} I_{q_r} \frac{L_m}{L_s} \quad (46)$$

$$Q_s = \frac{3}{2} V_{q_s} \left(\frac{\Psi_s}{L_s} - \frac{L_m}{L_s} I_{d_r} \right) \quad (47)$$

From eq46, 47 the required rotor currents are obtained and is compared with the measured value.

V. MODELLING OF THYRISTOR CONTROLLED REACTOR

Thyristor controlled reactor is a FACTS controller, in this case used to reduce the reactive power drawn by the DFIM WT. TCR basically consists of a pair of anti-parallel connected thyristor switches, out of which only one switch conducts during each half cycle of the AC supply. Another component SCR consists of is an air cored reactor.

A three phase basic thyristor based reactor is as shown in fig. 7. In power systems, TCR installations is of three phase. The additional components in TCR are filters and other

harmonic rejection components. Also, the inductors in the TCR will have small resistance. With this arrangement as shown in fig. 7 all the triplet harmonics are removed.

The working principle of TCR is that the conduction of the thyristor is controlled such that the required susceptance of the reactor to be connected to the system is controlled. By varying the susceptance of the reactor the reactive power of the system is controlled.

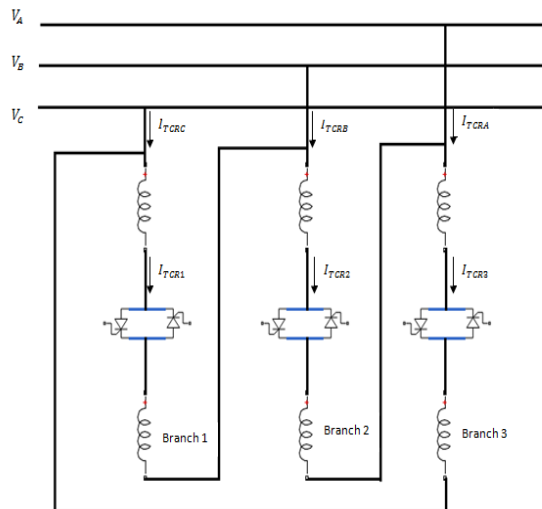


Figure 7. Three Phase Thyristor Controlled Reactor

The current through TCR and susceptance is given by eq. 48, 49 respectively

$$I_{TCR} = -jB_{TCR}V \quad (48)$$

$$B_{TCR} = \frac{2(\pi - \alpha) + \sin 2\alpha}{\omega L \pi} \quad (49)$$

For developing the mathematical model of TCR it is assumed that all the harmonics are eliminated and the main concern is with respect to fundamental frequency. From eq. 48 we can write

$$\begin{bmatrix} I_{TCR1} \\ I_{TCR2} \\ I_{TCR3} \end{bmatrix} = \begin{bmatrix} -jB_{TCR1} & 0 & 0 \\ 0 & -jB_{TCR2} & 0 \\ 0 & 0 & -jB_{TCR3} \end{bmatrix} \begin{bmatrix} V_1 \\ V_2 \\ V_3 \end{bmatrix} \quad (50)$$

And connectivity matrices for phases A, B, C are

$$\begin{bmatrix} V_1 \\ V_2 \\ V_3 \end{bmatrix} = \frac{(\pi/6)}{\sqrt{3}} \begin{bmatrix} 1 & -1 & 0 \\ -1 & 1 & -1 \\ 0 & -1 & 1 \end{bmatrix} \begin{bmatrix} V_A \\ V_B \\ V_C \end{bmatrix} \quad (51)$$

$$\begin{bmatrix} I_{TCRA} \\ I_{TCRB} \\ I_{TCRC} \end{bmatrix} = \frac{(-\pi/6)}{\sqrt{3}} \begin{bmatrix} 1 & 0 & -1 \\ -1 & 1 & 0 \\ 0 & -1 & 1 \end{bmatrix} \begin{bmatrix} I_{TCR1} \\ I_{TCR2} \\ I_{TCR3} \end{bmatrix} \quad (52)$$

Substituting eq. 50, 51 in 52. And assuming all the susceptance is equal i.e. $B_{TCR1} = B_{TCR2} = B_{TCR3} = B_{TCR}$

$$\begin{bmatrix} I_{TCRA} \\ I_{TCRB} \\ I_{TCRC} \end{bmatrix} = \frac{1}{3} \begin{bmatrix} -2jB_{TCR} & jB_{TCR} & jB_{TCR} \\ jB_{TCR} & -2jB_{TCR} & jB_{TCR} \\ jB_{TCR} & jB_{TCR} & -2jB_{TCR} \end{bmatrix} \begin{bmatrix} V_A \\ V_B \\ V_C \end{bmatrix} \quad (53)$$

Where I_{TCR} is the current through TCR; B_{TCR} susceptance of TCR; α is the firing angle.

VI. WIND TURBINE CONTROL USING PITCH ANGLE CONTROL

Pitch angle is the angle of attack of the blades of the propeller into or out of wind to control the production or absorption of power. Wind speed is highly unpredictable. The

range of wind speed that is required for wind energy conversion system is 5mps – 25mps. If the speed of wind is below 5mps, there is no sufficient wind energy to rotate the blades of the propeller. If the wind speed exceeds 25 mps, there will be mechanical vibrations generated. These vibrations transmit to the electrical part of the wind turbine causing failure of electrical components.

As wind speeds are unpredictable, a controller is required to control the speed of the rotor. This can be done by controlling the pitch angle of the blades of the propeller. This pitch angle varies from 2° to 40°. If the wind speed increases the pitch angle decreases and when the wind speed reduces pitch angle increases. The pitch angle control is achieved by implementing a PI controller. The method used to control the pitch angle is the speed of the generator rotor speed is compared to the reference speed. Error signal thus obtained is controlled using PI controller.

Depending on the generator power rating, the base speed of the wind turbine is determined using the graph shown in fig. 8. Once the value of base speed is obtained, the tip speed Ratio is determined.

A. Tip Speed Ratio

Tip speed ratio is the ratio of blade tip linear speed to wind speed. The power extracted from the wind by the wind turbine is determined by this factor. TSR is kept constant throughout the operation. TSR is calculated by using the eq. 48

$$Q_s = \frac{3}{2} V_{q_s} \left(\frac{\Psi_s}{L_s} - \frac{L_m}{L_s} I_{d_r} \right) \quad (54)$$

From the base speed the TSR is determined using the graph shown in fig. 9

B. Rotor Power Coefficient

Rotor power coefficient is a measure of rotor efficiency; it's the ratio of extracted power to the wind power.

$$C_p = \frac{\text{Extracted Power}}{\text{Power in Wind}} = \frac{P_{Rotor}}{P_{Wind}} \quad (55)$$

C_p Can be determined directly from the graph shown in fig. 10

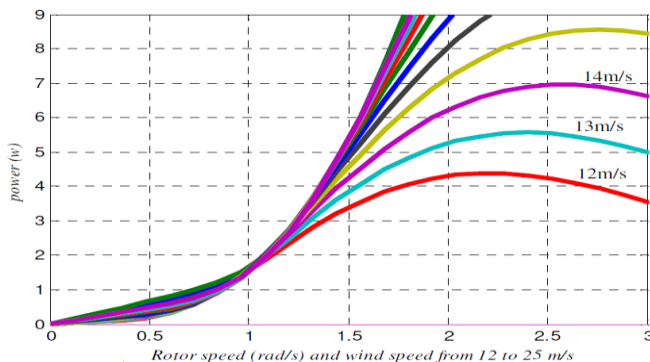


Figure 8. Generator Power Rating versus Rotor Speed

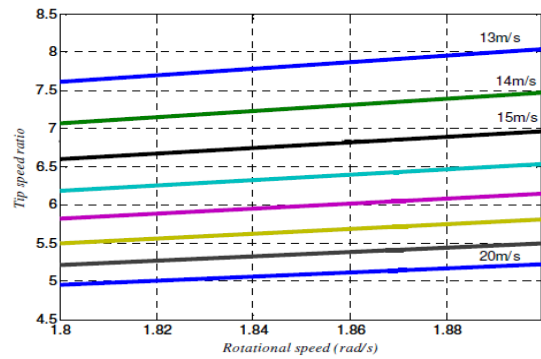


Figure 9. Tip Speed Ratio versus Rotational Speed

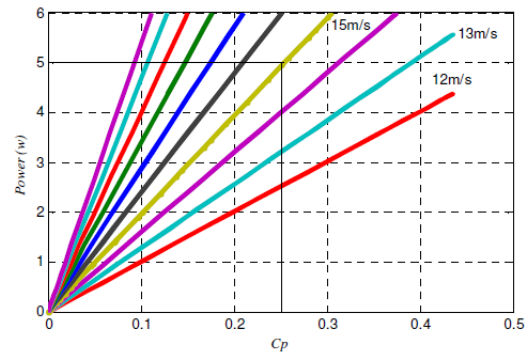


Figure 10. Generator Power Rating versus Rotor Power coefficient

VII. SIMULATION AND RESULTS

Table 1. Wind Turbine Subsystem Parameters

Generator power rating	5kW
Base wind speed	15 mps
Reference rotational speed	1.6 p.u.

Table 2. PI controller constants for pitch angle control

PI Controller Constants	Before tuning	After tuning
Proportional constant kp	1	854.26
Integral constant ki	1	113.19

As it can be seen in the above fig. 11 the wind speed is varied in steps for every 1 second of simulation. Simultaneously the pitch angle also varies automatically. This pitch angle control is done by PI controller. For higher speeds of wind the pitch angle decreases such that the speed of rotation of the propeller blades in wind turbine decreases and for lower speeds of wind the pitch angle increases such that the speed of rotation of propeller blades increases. It can be observed that, for wind speeds above 14m/s the pitch angle decreases and for below 14m/s pitch angle increases.

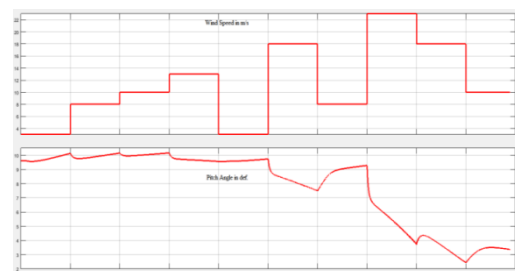


Figure 11. Wind Speed in mps and Pitch angle in deg.

Table 3. Base Power, Grid and Converter parameters

Base power	2MW
Base voltage	690Vrms
Base Current	966.1835 Irms
Base Angular Frequency	1500 rev/min
Grid Voltage Amplitude (phase)	400 V (690V L-L)
p.u. Grid Voltage Amplitude	1 p.u.
Frequency of Grid voltage	50 Hz
Converter Filter Inductor	50 μ H
Converter Filter Resistor	10 Ω

Table 4. DFIM characteristics

Synchronous speed	1500 rev/min
Rated Power	5kW
No. of poles	4
Turns ratio	0.54
R_s	0.72 Ω
R_r	0.75 Ω
L_s	91.6 mH
L_r	91.6 mH
L_m	85.8 mH
J	0.0226

Initial condition for DC link capacitor is set to 1p.u. i.e. it is assumed that capacitor is fully charged. Hence during simulation, the capacitor charges to its maximum potential of 0.8p.u. And not to 1p.u. This is because; batteries are not charged to its rated voltage or discharged to 0p.u. to increase its life cycle. The DC link capacitor is constant and remains at a value around 0.8p.u. As seen in fig. 12. At different settings of reactive power (0.9p.u and -0.9p.u) exchange also, the DC link voltage remains at a value around 0.8p.u. As shown in fig 13 and 14

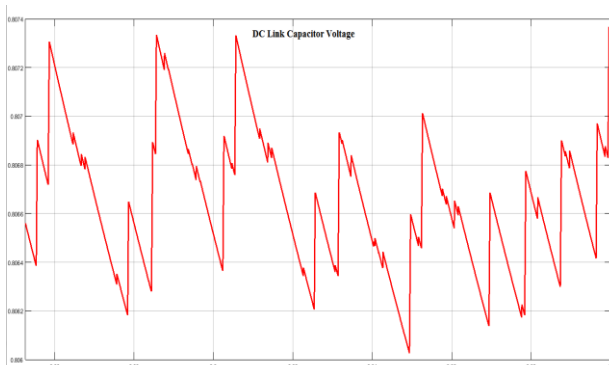


Figure 12. DC Link capacitor voltage at 0 p.u. reactive power setting zoomed in

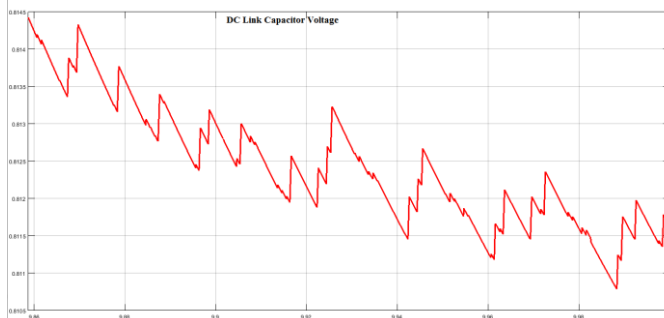


Figure 13. DC Link capacitor voltage at 0.9 p.u. reactive power setting

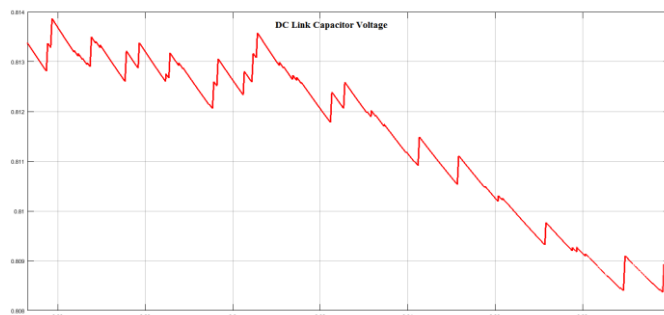


Figure 14. DC Link capacitor voltage at -0.9 p.u. reactive power setting

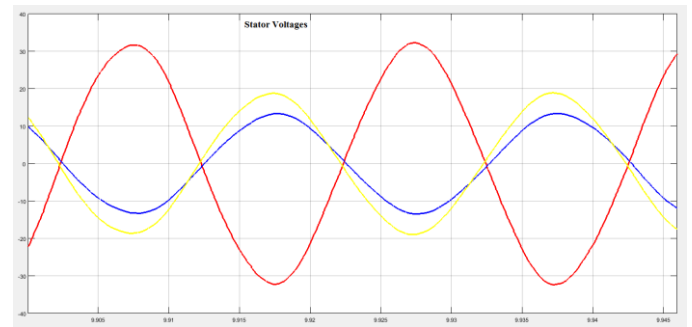


Figure 15. Stator voltages in p.u.

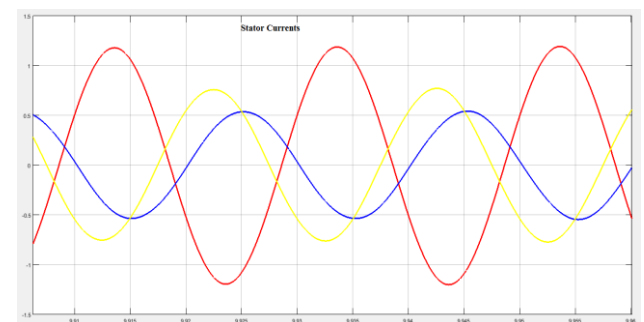


Figure 16. Stator currents in p.u.

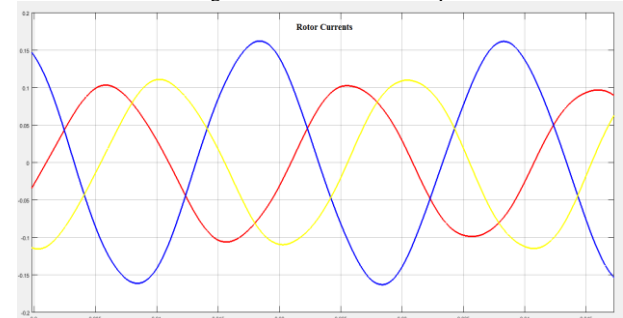


Figure 17. Rotor currents in p.u.

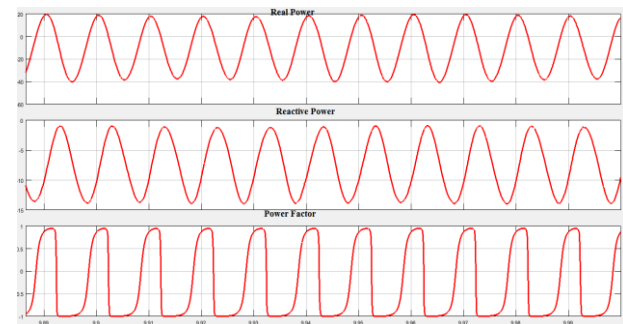


Figure 18. Real power, reactive power and power factor without TCR

In fig. 18 the reactive power is more, almost 50% of real power. The value of power factor varies between +1 and -1. By implementing thyristor controlled reactor, the reactive power is reduced and power factor takes a value of either +1 or -1 as shown in fig. 19.

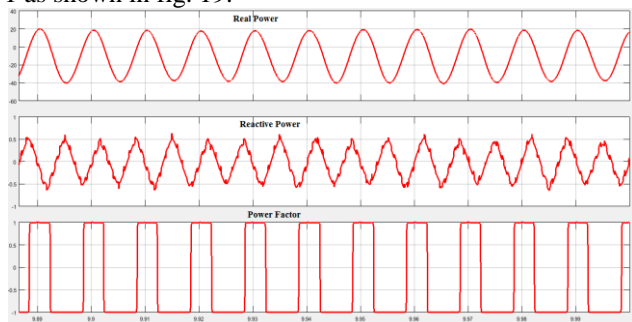


Figure 19. Real power, reactive power and power factor with TCR

VIII. CONCLUSIONS

Mathematical model of DFIM, two level voltage source and DC link capacitor is described individually. Grid side converter is controlled by grid voltage oriented vector control and third harmonic injection PWM scheme is been implemented. Back to back converter is checked for controlling DC capacitor voltage control satisfactory results are obtained. The rotor side converter is controlled with rotor current reference vector control. And a complete model of DFIM based wind turbine is modeled. The whole system is simulated for variable speed of wind and the pitch angle of the propeller blades is also controlled successfully. In order to overcome large reactive power drawing by DFIM, thyristor controlled reactor FACTS controller is modeled. With this reactive power control is done successfully.

REFERENCES

- [1] Nicholas W. Miller, Juan J. Sanchez-Gasca, William W. Price, Robert W. Price “*Dynamic Modelling of GE 1.5 and 3.6 MW Wind Turbine Generators For Stability Simulations*” IEEE WTG Modelling panel, p1977-1983, July 2003
- [2] Zhong Zheng, Geng Yang, Hua Geng “*Coordinated Control of a Doubly Fed Induction Generator-Based Wind Farm and a Static Synchronous Compensator for Low Voltage Ride Through Grid code Compliance during Asymmetrical Grid Faults*” *Energies Journal*, sept 2013
- [3] Stavros A. Papathanassiou “*Models for Variable Speed Wind Turbines*” PhD Thesis, NATIONAL TECHNICAL UNIVERSITY OF ATHENS School of Electrical and Computer Engineering Electric Power Division
- [4] Florin Iov, Anca Daniela Hansen, Poul Sørensen, Frede Blaabjerg “*Wind Turbine Blockset in Matlab/Simulink*” Institute of Energy Technology, Aalborg University, March 2004
- [5] D.Grahame Holmes Thomas A. Lipo “*Pulse Width Modulation for Power Converters Principles and Practice*” IEEE Series on Power Engineering, A JOHN WILEY & SONS, INC., PUBLICATION
- [6] BinWu Yongqiang, Lang Navid, Zargari, Samir Kouro “*POWER CONVERSION AND CONTROL OF WIND ENERGY SYSTEMS*” A JOHNWILEY & SONS, INC., PUBLICATION
- [7] Maurizio Cirrincione, Marcello Pucci, Gianpaolo Vitale “*Power Converters AC Electrical Drives with Linear Neural Networks*” CRC Press Taylor & Francis Group
- [8] Ned Mohan “*ADVANCED ELECTRIC DRIVES Analysis, Control, and Modeling Using MATLAB/Simulink®*” A JOHN WILEY & SONS, INC., PUBLICATION

- [9] Manuel Madrigal Martinez “*Modelling of Power Electronics Controllers for Harmonic Analysis in Power Systems*” A thesis submitted to the Department of Electronics and Electrical Engineering of The University of Glasgow for the degree of Doctor of Philosophy December 2001
- [10] Nguyen Phung Quang · Jörg-Andreas Dittrich “*Vector Control of Three-Phase AC Machines System Development in the Practice*”
- [11] Satish Choudhury, Kanungo Barada Mohanty, B. Chitti Babu, “*Performance Analysis of Doubly fed Induction Generator For Wind Energy Conversion System*” The 5th PSU-UNS International Conference on Engineering and Technology (ICET-2011), Phuket, pp. 532-536, 2-3 May 2011
- [12] Etienne Tremblay, Sergio Atayde, and Ambrish Chandra, “*Comparative Study of Control Strategies for the Doubly Fed Induction Generator in Wind Energy conversion Systems: A DSP-Based Implementation Approach*”, IEEE Transactions On Sustainable Energy, vol. 2, no. 3, pp. 288-299, July 2011.
- [13] Md. Rabiul Islam¹, Youguang Guo, Jian Guo Zhu, “*Steady State Characteristic Simulation of DFIG for Wind Power System*”, IEEE, 6th International Conference on Electrical and Computer Engineering ICECE, Dhaka, Bangladesh, pp. 151-154, 18-20 Dec. 2010.
- [14] <http://energy.gov/eere/wind/advantages-and-challenges-wind-energy>
- [15] http://www.mpoweruk.com/wind_power.htm